PAPER

Check for updates

The dermacozines and light: a novel phenazine semiquinone radical based photocatalytic system from the deepest oceanic trench of the Earth†

Bertalan Juhasz, [iD] [a] Angel Cuesta, [iD] [b,c] Russell F. Howe [iD] [b] and Marcel Jaspars [iD] *[a]

Dermacozines, the secondary metabolites of the Mariana Trench sediment bacterium *Dermacoccus abyssi* MT1.1[T], were studied using cyclic voltammetry (CV), electron paramagnetic resonance (EPR), furthermore literature and own experimental UV-Vis spectroscopic data. With those measurements, we determined experimentally the positions of the HOMO, which shifts towards more positive potentials, and the constant LUMO on the standard hydrogen electrode scale, while the HOMO–LUMO gap gets deeper, respectively. The HOMO energies of dermacozines experimentally were proven to be water oxidising. EPR spectroscopy demonstrated the formation of semiquinone radicals in the case of dermacozines E and O upon irradiation with visible light corresponding to the absorption maxima (AM) of the chromophores. Our findings suggest that the dermacozines may assist the strain by maintaining redox homeostasis through its respiratory chain.

1. Introduction

The piezotolerant and halotolerant actinobacteria *Dermacoccus abyssi* MT1.1[T] and MT1.2 were isolated from sediments originating from the deepest part of the Earth, the Challenger Deep, Mariana Trench, at 10 898 m depth.[1] These strains produce novel phenazine secondary metabolites: dermacozines A–G, dermacozines H–J, and dermacozines M–P [Fig. 1, ref. 2–5 and ESI S1†]. The *in vivo* function of these compounds is unknown, but it has been suggested that due to their range of UV-Vis absorbances, structural properties and radical scavenging activity they may participate in electron shuttling reactions.[2–5] Reports on phenazines participating in reducing matter (*e.g.*, $O_2/O_2^{\bullet-}$, Fe^{3+}/Fe^{2+}, Ag^+/Ag) are widespread in the literature.[6–9] The electrons for these reduction processes in heterotrophic bacteria originate from the Entner–Doudoroff pathway and the Szent-Györgyi–Krebs cycle.

Energy stored as NADH produced in these processes is released by oxidation back to NAD^{+}. Under microaerobic/anoxic conditions this process is supported by phenazines and is shown to assist the survival of *Pseudomonas aeruginosa* by maintaining redox homeostasis.[10] In *Phellinus noxious* mitochondria the role of PCA, the simplest carboxylated phenazine derivative, seems to be supported by its inductive effect on the gene expression of the cytochrome *a* enzyme complex,
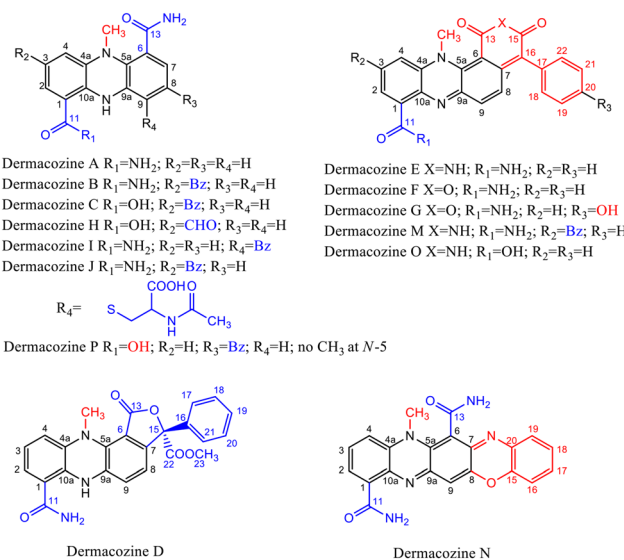

Dermacozine A R_1=NH$_2$; R_2=R_3=R_4=H
Dermacozine B R_1=NH$_2$; R_2=Bz; R_3=R_4=H
Dermacozine C R_1=OH; R_2=Bz; R_3=R_4=H
Dermacozine H R_1=OH; R_2=CHO; R_3=R_4=H
Dermacozine I R_1=NH$_2$; R_2=R_3=H; R_4=Bz
Dermacozine J R_1=NH$_2$; R_2=Bz; R_3=H

Dermacozine E X=NH; R_1=NH$_2$; R_2=R_3=H
Dermacozine F X=O; R_1=NH$_2$; R_2=R_3=H
Dermacozine G X=O; R_1=NH$_2$; R_2=R_3=H
Dermacozine M X=NH; R_1=NH$_2$; R_2=Bz; R_3=H
Dermacozine O X=NH; R_1=OH; R_2=R_3=H

R_4=

Dermacozine P R_1=OH; R_2=H; R_3=Bz; R_4=H; no CH$_3$ at *N*-5

Dermacozine D

Dermacozine N

Fig. 1 Dermacozine structures, and their electron-withdrawing and electron-donating substituents (EWG and EDG).[2–5]

[a]Marine Biodiscovery Centre, Department of Chemistry, University of Aberdeen, Meston Building, Aberdeen AB24 3UE, Scotland, UK. E-mail: m.jaspars@abdn.ac.uk, angel.cuestaciscar@abdn.ac.uk

[b]Advanced Centre for Energy and Sustainability (ACES), Department of Chemistry, University of Aberdeen, Aberdeen AB24 3UE, Scotland, UK

[c]Centre for Energy Transition, University of Aberdeen, Aberdeen AB24 3FX, Scotland, UK

increased reactive oxygen species (ROS) production, and the hyperpolarisation of the mitochondrial membrane potential ($\Delta\Psi_m$).[11] PCA and other phenazine derivatives reportedly can have an impact on the mitochondrial function.[11,12] These findings from the related literature overall indicate participation of PCA in an electron exchange reaction between the respiratory chain (ETC) components and the terminal electron acceptor (O_2) as an electron shuttle while reactive oxygen species (ROS) are produced. Phenazine-methosulphate (PMS) has been described as one of the most effective electron acceptors among the tested materials in the reaction from succinate to fumarate in the presence of soluble succinate dehydrogenases (SDHs) from a variety of sources.[13] SDH is the only enzyme complex (complex II) directly connecting the Szent-Györgyi–Krebs cycle to the respiratory chain in a way that it catalyses the oxidation of succinate to fumarate, where the electrons originating from succinate reduce ubiquinone (UQ) to ubiquinol (UQH_2). In the next step of the ETC these electrons would be conducted to cytochrome *c* (complex III). Furthermore, PMS was reported to be capable of accepting electrons from other ETC components downstream from complex II.[14] In rapid-freeze EPR studies PMS could re-oxidise all the detectable paramagnetic Fe–S 1 and HiPIP (high potential cluster) Fe–S centre species of complex (II) even at 0 °C within <6 ms.[15] Our group recently sequenced the whole genome of *Dermacoccus abyssi* MT1.1[T] and found SDH to be expressed in multiple copies.[4] In the study of Park *et al. Actinobacillus succinogenes* was capable of utilising reduced neutral red (NR), a synthetic phenazine, as the sole electron source to reduce fumarate to succinate.[16] Harrington *et al.* demonstrated in an *Escherichia coli* bioelectrochemical system that reduced NR oxidation occurs through the menaquinone pool in the inner bacterial membrane.[17] Since all phenazines are known to be redox active compounds, the structurally closely related dermacozines likely possess similar properties, capable of electron shuttling between the bacterial ETC and terminal electron acceptors. In this article we investigate their physicochemical behaviour especially focusing on their redox activity.

2. Results and discussion

2.1. The dermacozine HOMO–LUMO gap energies and dermacozine radicals

Dermacozines are colourful molecules [ESI S2†]. The experimental HOMO–LUMO gaps, as estimated from the absorption maxima in the visible absorption spectra of the isolated dermacozines in ethanol, are between 3.4 eV and 1.7 eV [ESI S3 and 4†]. *Dermacoccus abyssi* MT1.1[T] and 1.2 create these compounds *via* the shikimic acid pathway. In this process the electronic core phenazine structure is modified by the bacterium suggestive of compounds with differing redox properties.[2–5] To investigate this, we recorded CVs of test compounds isolated from the medium of *Dermacoccus abyssi* MT1.1[T] (dermacozines B, E, F, O, P and phenazine-1-carboxylic acid (PCA)) in a suit-

Table 1 Experimental anodic and cathodic potentials and electrochemically derived HOMO–LUMO gaps of dermacozines B, E, F, O and PCA in Volt $\pm$ SE (RE: Ag, acetonitrile, 0.1 M NaClO$_4$)

	Cathodic potential [V]	Anodic potential [V]	Electrochemically derived HOMO–LUMO gap [V]
Dermacozine B	-0.85 ± 0.05	$+1.27 \pm 0.02$	2.12 ± 0.05
Dermacozine E	-0.89 ± 0.02	$+1.01 \pm 0.02$	1.91 ± 0.03
Dermacozine F	-0.83 ± 0.02	$+1.17 \pm 0.01$	2.00 ± 0.02
Dermacozine O	-0.88 ± 0.01	$+0.88 \pm 0.00$	1.76 ± 0.01
PCA	-0.96 ± 0.02	$+1.29 \pm 0.03$	2.25 ± 0.03

able electrolyte (0.1 M NaClO$_4$ in acetonitrile) [ESI S5–10† and Table 1].

The first redox process in the negative-going potential sweep (cathodic $\varepsilon_{1/2}$) must correspond to injection of one electron into the LUMO of the compound, and therefore reflects the position of the LUMO. Similarly, the first redox process in the positive-going potential sweep (anodic $\varepsilon_{1/2}$) must correspond to removing one electron from the HOMO of the compound, and therefore reflects the position of the HOMO. The separation between them must hence correspond to the HOMO–LUMO gap in eV. The CV of dermacozine B shows a clear reduction shoulder visible around -0.9 ± 0.1 V. A shoulder around $+1.3 \pm 0.0$ V can also be observed in the exponentially growing current at the positive potential limit which signals the decomposition of the solvent. This would yield an electrochemically derived HOMO–LUMO gap of 2.1 ± 0.1 V [ESI S5, S11† and Table 1]. These processes lack the corresponding counter peaks, implying that the radical cation and anion that result from the oxidation and reduction, respectively, undergo fast subsequent reaction(s). In fact, upon cycling new peaks appear in the central region of the CVs, the intensity of which decreases with increasing scan rates. The cathodic and anodic peaks and the resultant electrochemically derived HOMO–LUMO gaps are similarly identifiable on the CVs of dermacozines E, F, O and PCA, respectively, as demonstrated in Table 1.

Dermacozine P's anodic and cathodic peaks overlap too much with the decomposition of the solvent, and therefore they were disregarded in subsequent calculations [ESI S10†].

A plot of the electrochemically derived gap of the isolated dermacozines *vs.* the corresponding maximum in the UV-vis absorption spectra is linear with $R^2 = 0.92$ ($p = 0.01$). Therefore, CV provides evidence that the redox order of dermacozines determined by UV-Vis spectroscopy[2–5] is correct [ESI S3, S4 and S12a, S12b†]. A linear correlation [ESI S13a and S13b†] is also obtained when the optically determined HOMO–LUMO gaps of dermacozine B, E, F, O and PCA are plotted against the anodic $\varepsilon_{1/2}$ in the corresponding CV. No significant correlation was found, however, between the optically determined HOMO–LUMO gaps and the cathodic $\varepsilon_{1/2}$ in the CVs of these dermacozines (*i.e.*, E_{LUMO} = constant) [ESI S14a and S14b†]. This allowed us to conclude that the LUMOs must be approximately at the same energy, and that the increase in the HOMO–LUMO gaps is due to the HOMO gradu-

ally shifting to deeper energies (*i.e.*, more positive potentials) [Fig. 2]. Based on the constant LUMO energies, the arithmetic mean of the measured cathodic potentials was considered ± ME [ESI S11†].

The anodic $\varepsilon_{1/2}$ ± ME values of those other known dermacozines, for which we could not obtain CVs (dermacozines A, C, D, G, H, I, J, M, and N were not isolated), were approximated by interpolation using the found linear relationship and the value of the band gap obtained by optical measurements and the measured anodic potentials ± SE [please see ESI S11 and S13†].

The potential difference between the Ag pseudo-reference electrode and the standard hydrogen electrode (III) was calculated based on the potential difference detailed in (I) and (II) as follows:

$$\mathrm{Ag/AgCl\,(3\,M\,KCl_{aqu.})\parallel Ag\,(0.1\,M\,NaClO_{4\,ACN})} \quad \varepsilon = +0.162\,\mathrm{V} \tag{I}$$

$$\mathrm{Pt\,(1\,M\,H^+/H_2\,(1\,atm))\parallel Ag/AgCl\,(3\,M\,KCl_{aqu.})}$$
$$\varepsilon^{\circ} = +0.197\,\mathrm{V} \tag{II}$$

$$\mathrm{Pt\,(1\,M\,H^+/H_2\,(1\,atm))\parallel Ag\,(0.1\,M\,NaClO_{4\,ACN})}$$
$$\varepsilon^{\circ} \cong +35\,\mathrm{mV} + E_{\mathrm{L.-J.}} \tag{III}$$

The Ag/AgCl (3 M KCl$_{aqu.}$) electrode potential experimentally turned out to be +0.162 ± 0.003 V more positive than that of the Ag wire in 0.1 M NaClO$_4$ acetonitrile. With this value the calculated anodic and cathodic potentials were attempted to be translated to the standard hydrogen electrode [ESI S11†]. This implies, based on our experimental data, that the Ag wire in acetonitrile is approx. 35 mV more positive than the H$^+$/H$_2$ couple under standard conditions ($\varepsilon_{\mathrm{III}}^{\circ} \cong \varepsilon_{\mathrm{II}} - \varepsilon_{\mathrm{I}}^{\circ}$). Fourmond *et al.* estimated the H$^+$/H$_2$ couple to be −70 mV

compared to the Fc^0/Fc$^+$ equilibrium potential in acetonitrile, which approximates the H$^+$/H$_2$ couple to be 33 mV more negative in acetonitrile than the Ag/AgClO$_4$ electrode.[18,19] Even though in our experiments an Ag pseudo-reference electrode was immersed in acetonitrile, our value is reasonably in agreement with the literature. Although, as the main theoretical limitation of our study, we must note that there is still a considerable uncertainty with regards to the absolute value of the $\varepsilon_{\mathrm{SHE}}^{\mathrm{ACN}}$. The above approximated value of $\varepsilon_{\mathrm{SHE}}^{\mathrm{ACN}}$ shows 0.1–0.2 V difference *versus* the calculated values reported by Fawcett.[20]

De la Cruz *et al.* also reported that in DFT modelled studies the predicted redox potential shifts in the case of a parent phenazine as an analyte, between solvent systems having a higher dielectric constant than $\varepsilon_{\mathrm{r}} > 20$ (*e.g.*, acetonitrile and water), are within approximately ∼0.1 V and a similar trend is expected for other phenazine derivatives as well.[21] Furthermore, the *N*-alkylated phenazines are oxidised and reduced involving 1 e^-/1 H$^+$ steps in their redox reactions.[22,23] Taking these literature data and the liquid–junction potential [$E_{\mathrm{L.-J.}}$ in (III), and ESI S11†] into consideration, not only the electrochemically derived HOMO–LUMO gaps of dermacozines but the absolute values of their anodic and cathodic potentials need to be reasonably in good agreement with the absolute SHE scale to our approximated potential values of dermacozines *versus* SHE.
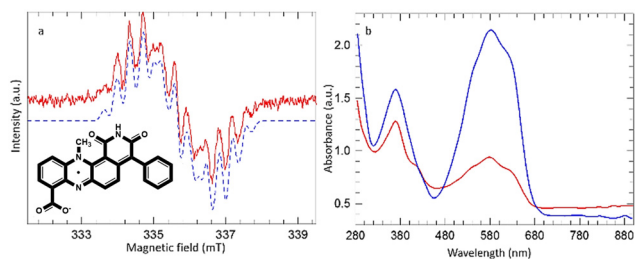
Dermacozines with electron-withdrawing substituents (EWG) possess larger HOMO–LUMO gaps (PCA and dermacozines A, B, C, D, H, I, J, P), whereas dermacozines with electron-donating functionalities (EDG) (dermacozines E, F, G, M, N and O) have shallower gaps [ESI S1, 3, 4† and Fig. 1]. The resultant interpolated anodic potentials *vs.* SHE are in keeping with the previously published experimental data – based on DPPH• radical scavenging assays – that dermacozines with larger optical HOMO–LUMO gaps: dermacozines C, H, J, I, B, A, and D can act as antioxidants, in this order, with dermacozine C possessing the highest antioxidant activity. Structures of the type represented by E, F, and G (Fig. 1) do not participate in that particular radical scavenging activity. This experimental fact serves as independent evidence for the validity of our experimental data detailed in this paper.[2,3]

The wide range visible AMs obtained in our and previous studies with dermacozines have stimulated our interest, whether an excitation process in the visible electromagnetic spectrum (EM) could provide activation energy and could make these compounds oxidised/reduced.[2–5] Therefore, we irradiated PCA, dermacozines E, P and O through a coloured filter corresponding to their AM in the visible EM spectrum. The resultant EPR signals detected in the case of dermacozines E and O provided evidence for the existence of their related semiquinone paramagnetic species [Fig. 3, 4 and ESI S15–17†]. Dermacozines P and B were only soluble in acetonitrile or methanol but not in chloroform. As a consequence, the EPR spectrometer could not be tuned to visualise whether their corresponding semiquinone radicals form or not. In the case of dermacozine F we had insufficient amount of material left after the CV experiments.
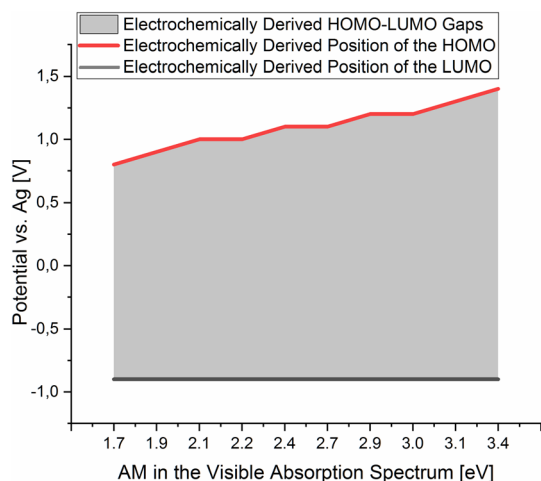

Fig. 2 The positions of the HOMO and LUMO of the isolated dermacozines on the Ag quasi-reference electrode scale were obtained from the corresponding cyclic voltammograms in 0.1 M NaClO$_4$ in acetonitrile. These data points were plotted against the absorption maxima of the visible absorption spectra of the dermacozines in ethanol. The grey shaded area corresponds to the HOMO–LUMO energy gaps resulting from the electrochemical experiments.

6158 | *Org. Biomol. Chem.*, 2024, **22**, 6156–6165

This journal is © The Royal Society of Chemistry 2024

Fig. 3 (a) EPR spectrum obtained upon irradiation of dermacozine O in chloroform at 550 ± 50 nm. The blue dashed line is simulated with parameters described in the text. (b) UV-Vis spectra of dermacozine O in chloroform before (blue) and after (red) irradiation at 550 ± 50 nm (inlet: dermacozine O neutral semiquinone radical).
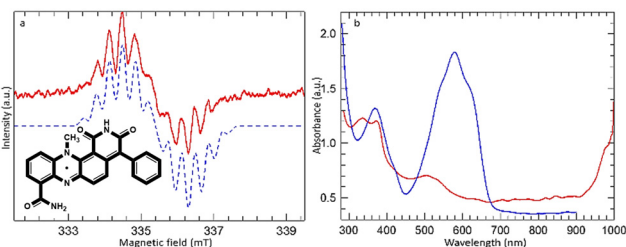
Fig. 4 (a) EPR spectrum obtained during irradiation of dermacozine E in chloroform at 550 ± 50 nm. The blue dashed line is simulated with parameters described in the text. (b) UV-Vis spectra of dermacozine E in chloroform before (blue) and after (red) irradiation at 550 ± 50 nm (inlet: dermacozine E neutral semiquinone radical).

In the case of dermacozine O a stable radical was detected when its chloroform solution was irradiated at 550 ± 50 nm. Fig. 3(a) shows the EPR signal obtained, and Fig. 3(b) shows the comparison of the UV-Vis spectra of dermacozine O before and after irradiation at 550 ± 50 nm. Irradiation caused a colour change from blue to light blue [ESI S15 and 17–19†]. The EPR signal obtained from dermacozine O comprises at least 13 lines with an average splitting of ~0.4 mT. The signal was satisfactorily simulated using parameters adapted from those reported by Catallo *et al.* for the methyl phenazine radical.[24] These authors generated the neutral methyl phenazine radical by electrochemical reduction of phenazine methosulphate in aqueous media to form the protonated cation radical followed by extraction of the deprotonated neutral radical into toluene.

The 14-line hyperfine structure observed for the methyl phenazine radical was attributed to coupling to 2 inequivalent ^{14}N nuclei (0.70 and 0.43 mT), 3 methyl protons (0.47 mT), and 2 sets of 4 equivalent protons on the two adjacent aromatic rings (0.36 mT and 0.065 mT). In the dermacozine O radical there are only 2 adjacent apical protons. The simulated spectrum in Fig. 3(a) used the following parameters: ^{14}N 0.625 and 0.450 mT, 3 methyl protons 0.39 mT, and 2 adjacent apical aromatic protons 0.27 mT. Any coupling from the remaining adjacent aromatic protons was too small to be

resolved within the simulated line width of 0.23 mT. The dermacozine O radical once formed was stable at room temperature and on exposure to atmospheric oxygen. When a 5 µL water aliquot was added to ~100 µL chloroform dermacozine O solution the AUC approximately doubled suggesting a reaction between the exciton in chloroform solution and water. However, further irradiation after addition of water caused immediate loss of the EPR signal [ESI S15†].

A similar EPR signal was obtained when dermacozine E was irradiated with a 550 ± 50 nm light filter [ESI S16† and Fig. 4]. However, the radical produced in this case was unstable to further irradiation and was totally lost after ~1 hour of irradiation. The spectrum shown in Fig. 4(a) was recorded after 30 minutes of irradiation; the apparent asymmetry of the signal reflects its partial loss during the scan.

Simulation of the signal of dermacozine E could be achieved with slightly smaller ^{14}N coupling constants (0.605 and 0.405 mT) but with the same proton coupling constants as for the dermacozine O radical *i.e.*, this is also the neutral semiquinone radical. The sample initially changed colour from blue to green but after further irradiation it turned orange [ESI S16, S20 and 21†]. Fig. 4(b) shows the comparison of the UV-Vis spectrum of dermacozine E in chloroform before and after irradiation. The appearance of an intense band beyond 1000 nm could be completely reversed by subsequent addition of methanol to the solution, which fully restored the blue colour and the absorption spectrum of dermacozine E. LC-(HR)-ESI-MS^n (MF = $C_{23}H_{16}N_4O_3$) and UV-Vis spectroscopy confirmed that dermacozine E is responsible for the appearance of the blue colour [ESI S22 and 23†]. No chlorine abundance pattern was revealed in the MS spectra, which excluded the possibility of the radical reacting with chloroform [ESI S23–25†].

The appearance of a near-infrared absorption band in the spectrum of *N*-ethyl-phenazine on cooling below room temperature has been attributed to the formation of dimeric species in Birkofer and Hausser results.[25,26] We speculate that the "instability" of the dermacozine E semiquinone radical is due to the dimerization of the paramagnetic compound, while reaction with methanol restores the original dermacozine E molecule. Birkofer and Hausser reported dimer formation of the *N*-ethyl-phenazine radical when the solution of the *N*-ethyl-phenazine radical was cooled to 80 K. Since in the case of dermacozine E it happens at 298 K, the dimerization energy of the dermacozine E semiquinone radical must have overcome the *kT* thermal disorder [ESI S20–24†]. The experimental fact that dimerization does not happen in the case of dermacozine O can be explained plausibly by its deprotonated state in non-acidified chloroform solvent by being a strong acid,[5] and therefore the stronger Coulomb repulsion between the deprotonated carboxylate functionalities exceeds the dimerization tendency.

The dermacozine E radical does not form without visible light irradiation and in the absence of water. In meticulously dried samples the EPR signal cannot be detected in the case of dermacozine E even following excitation with its AM. But by

This journal is © The Royal Society of Chemistry 2024

Org. Biomol. Chem., 2024, **22**, 6156–6165 | **6159**

adding around 5 μL of water aliquot to the same sample while being irradiated through a 550 ± 50 nm filter, the experiment will result in the formation of the dermacozine E semiquinone paramagnetic species. It proves that visible light illumination with a specific activation energy makes these compounds paramagnetic *via* an excitation process. Furthermore, it also gives some indication that there is a redox reaction between water and the dermacozine E exciton in chloroform solvent. The O_2/H_2O couple redox potential at pH 7 is +0.81 V. If the dermacozine E redox reaction with water was not proton coupled, this value will always be more negative at pH 7 than the dermacozine E $(\varepsilon^\circ_{ox} = +1.0 \pm 0.01\,V)_{calc.}$ and O oxidation potential $(\varepsilon^\circ_{ox} = +0.9 \pm 0.01\,V)_{calc.}$. Since dermacozine E and O EPR spectra have shown that the *N*-10 nitrogen atoms in their structures are not protonated and their radicals are neutral (Fig. 3 and 4), it is likely that their redox potential is independent of pH (as opposed to the reduced structures with anodic potentials more positive than ~+1.2 V. 90–99% of these compounds get protonated under pH values lower than their pK_a) [ESI S11†]. The anodic potentials of the dermacozines with an oxidised type of phenazine skeleton (N, O, M, G, E, F) are all non-pH dependent based on high structural similarity to dermacozines E and O [Fig. 2, ESI S1† and ref. 2, 4, 5]. Therefore, upon the h^+ hole formation following visible EM excitation, they should be able to oxidise water at pH 7. This would provide a plausible explanation for our EPR experimental observations with water following excitation as detailed above.

Oxidation of water likely will result in ROS production. The bacterium possesses catalase, superoxide-dismutase (SOD), thioredoxin-disulphide reductase, thioredoxin, peroxiredoxin, NAD(P)H-quinone oxidoreductase, arsenate reductase, alkyl hydroperoxide reductase, glutathione *S*-transferase and glutaredoxin enzymes and as such should be capable of handling higher hydrogen-peroxide and ROS levels, while diatomic O_2 is produced.[4] Diatomic oxygen production would be useful for the bacterium under microaerobic/anaerobic conditions such as the mud at the depth of the hadal zone. H_2O_2 production in nature is primarily photochemical, and therefore, its nanomolar concentration under the continental shell – up until solar photons are abundant – is not explained.[27] In the deep oceans the production rate of H_2O_2 is ~0.8–9 pM h^{-1} and the most likely source is bacterial metabolism.[27] *Dermacoccus abyssi* MT 1.1^T and MT 1.2 potentially belong to those species capable of producing H_2O_2 at that depth. In the Mariana Trench the oxygen concentration was reported to be 3.07–4.42 mL L^{-1}.[28] In the mud at the bottom the oxygen concentration is likely considerably less.

Since the energy levels of the LUMO orbitals of dermacozines are constant, whilst their HOMO energies are stepwise increasing/decreasing (Fig. 2) – considering that Kenichi Fukui's frontier orbital theory can be applied to radical reactions – it is possible that they can shuttle electrons between each other.[29] In principle, based on our SHE referenced electrochemistry data [ESI S11†], the oxidation reactions can even be coupled to the ETC of the bacterium itself. Dermacozine N, with the least positive predicted oxidation

potential isolated to date $(\varepsilon^\circ_{ox} = +0.8 \pm 0.01\,V\,(SHE)_{calc.}$ in acetonitrile), is more positive than the benzoquinone/hydroquinone redox couple in the same solvent system with reference to SHE.[30] Franco *et al.* concluded that phenazines play a pivotal role in electron transport between the ETC and terminal oxidases, mainly through NADH dehydrogenases; they also noted that phenazines cannot replace oxygen respiration in biomass formation.[31] Sinha *et al.* described that NADPH alone or in conjuncture with cytP$_{450}$ reductase in the presence of 1-OH-phenazine increased the level of ROS, where NADPH is oxidised.[9]

As previously mentioned, phenazines coupled to ETC enzyme redox reactions are well known. In addition to that experimental fact, our study suggests that those reactions might even be influenced by visible photons *in vitro*. Phenazine type structures are known to produce semiquinone radicals upon excitation with light.[32] Zaugg *et al.* reported light induced direct electron transfer during the photophosphorylation reaction between *Rhodopseudomonas rubrum*, *R. spheroides* and *chromaticum* chromatophores and PMSH$_2$, where UQ is reduced and PMS is oxidised.[33] The function of dermacozines is not expected to be connected to visible photons, since in the bacterium's natural habitat, in the hadal zone, there is no visible EM of solar origin. Their rainbow colours observed during their isolation process in our study are somehow suggestive of them participating in optical physicochemical phenomena [ESI Fig. S2†]. The existing DFT computational chemistry reports predict large non-linear optical susceptibilities upon laser excitation, where all dermacozines showed high values at 800 nm, and particularly the dermacozine E, F, G-like structures displayed very large hyperpolarizabilities at 1064 nm.[34] Although at the mesmerizing depth of deep oceans visible photons reportedly exist from sources like the β$^-$ emitting ^{40}K decay to the ^{40}Ca stable isotope, bioluminescence, chemiluminescence, black smokers, and seismic light,[35,36] significant participation of light in the biological function of dermacozines due to the published low abundance of these photons is unlikely. Even if it was possible for the organism to make oxidising dermacozine radicals with light at that depth, this process will likely not participate in biomass formation in the hadal zone due to the same considerations.

Since there are more than 6000 synthetic phenazines and more than 100 phenazines of natural origin, our report may open new horizons for influencing ETC reactions with phenazines at the molecular level with photons corresponding to their AMs in the visible EM spectrum.

2.2. Potential applications of dermacozine radicals

Oxidising/reducing substrates with the energy of photons is a well established practice in photocatalysis. Phenazines' redox properties were found to be useful in shuttling electrons between enzymes or electrodes. The electrical properties of electron-mediators (MEDs, redox active molecules capable of mediating electron transfer) are exploited in biological reactions, photocatalysis or manufacturing *e.g.*, Li–O$_2$ batteries.[37] De la Cruz *et al.* predicted through computational chemistry

6160 | *Org. Biomol. Chem.*, 2024, **22**, 6156–6165

This journal is © The Royal Society of Chemistry 2024

calculations that the redox potentials of phenazines can be modified with electron-withdrawing (EWG) and electron-donating functionalities (EDG), where EDGs shift their redox potentials towards more negative and EWG functionalities towards more positive values.[21] This concept was experimentally demonstrated in our manuscript. Dermacozines with their similar wide range of redox potentials could be suitable candidates for conducting further MED and redox-flow battery (RFB) studies.

Considering that dermacozines are reportedly compounds with cytotoxic activities against chronic myelogenous leukaemia (K562), aggressive melanoma (A2058) and hepatocellular carcinoma (HepG2) cells, and their synthetically modulated derivatives exhibit even stronger anti-tubulin *in vitro* activity than the nocodazole control, the discovery of dermacozines' photo-redox properties may provide interesting redox active mechanisms for anti-cancer drug discovery in medicinal chemistry.[5,38,39]

Photosensitisation and photo-dynamic-Therapy (PDT) acting through generating ROS is a promising technique utilised in the treatment of cancer, viral-, bacterial-, and fungal infections, cardiovascular diseases, and dermatological conditions, with *e.g.*, no reported antimicrobial resistance so far mentioned in the literature.[40] Incorporating photosensitised substances into nanostructures (*e.g.*, copolymeric micelles, liposomal vesicles, nanosuspensions *etc.*) provides protection against biological breakdown, improves bio-transport and due to amplified bioavailability potentiates action at the site of action.[41,42] Most antibacterial and anticancer studies related to phenazines were reported in darkness.[40] There are only a few phenazines which were reported to be PDT active following visible light illumination, *e.g.*, white light illuminated (Hg lamp) safranin O and Au nanoparticles incorporated into copolymer emulsion paint caused more lethal photosensitisation of *Escherichia coli* and *Staphylococcus aureus*, and possessed less toxic effect under dark conditions.[41] In another study neutral red delivered with thioglycolate covered Au nanoparticles and illuminated with a $\lambda = 440$ nm Twin Flex LASER LED MMoptics system led to reduced cell viability of NIH-3T3 fibroblast and 4T1 tumour cell lines.[42] None of these compounds were prepared as stable radicals with illumination prior to being tested against pathogens/cancer cell lines.[40–42] The activity of dermacozines based on their water oxidising redox potentials in our work might be augmented with light, where their radicals may become more potent anticancer agents in nature.

3. Conclusion

The coloured dermacozines' UV-Vis, CV and EPR data demonstrated that their energy levels can be influenced with visible photon excitation. Utilising this theory, we have observed the existence of two paramagnetic dermacozine species: the neutral dermacozine E and O semiquinone radicals. The HOMO energies of dermacozines increase in parallel with a decrease in the HOMO–LUMO band gap, which implies that

their LUMO energy is constant. Respectively, from the interpolated electrode potentials, the position of the cathodic potential was found to be the same, -0.9 ± 0.02 V, for all dermacozines, whereas the anodic potentials were between $+0.8 \pm 0.01$ V and $+1.4 \pm 0.01$ V, and consequently the electrochemically derived band gaps grew larger.

In principle the anodic potentials of dermacozines can be connected to the benzoquinone/hydroquinone redox couple since it's redox potential (SHE) in the same solvent system turned out to be more negative than that of dermacozine N, the dermacozine isolated to date with the least positive anodic potential (SHE). Nevertheless, there are examples of phenazines capable of accepting electrons in the succinate–fumarate oxidation process through SDH, which is expressed in *Dermacoccus abyssi* MT1.1[T] in multiple copies. As such, we propose that the dermacozine redox system can shuttle electrons from the respiratory chain of *Dermacoccus abyssi* MT1.1[T] and MT1.2, and it conducts them to a final electron acceptor.

Our CV measurements have shown that the HOMO energy levels of dermacozines are water oxidising in acetonitrile solvent and 0.1 M $NaClO_4$ conducting electrolyte. In addition to this experimental fact, our EPR experiments with the dermacozine E and O semiquinone radicals in chloroform solvent were suggestive of water oxidation as well, whilst the required activation energy was gained from a visible light source with a frequency corresponding to the absorption maxima of these dermacozines in the visible EM.

Our study may lead to new research ideas in physical chemistry, medicinal chemistry, and redox chemistry in the future, where the properties of these photo-redox active compounds and their radicals can be further investigated and utilised *e.g.*, in photocatalysis, photo-redox chemistry, and photodynamic therapy (PDT). Other phenazines should behave in the same way as dermacozines, and therefore they may provide photo-redox access to ETC components and more potent photo-sensitive anticancer drugs in the future.

4. Materials and methods

4.1. Organism

Mariana Trench sediment was collected from the Challenger Deep (11°19′911″N; 142°12′372″E) on the 21st of May 1998 during dive number 74 by the JAMSTEC team with the remotely operated submersible Kaiko. The sample (2 mL) was transported at $+4$ °C in an insulated container to the UK and stored at -20 °C. The strain was isolated with raffinose-histidine agar supplemented with cycloheximide and nystatin.[1] The pure colony of the strain was received from the School of Biology, University of Newcastle, on an ISP2 agar plate and kept in (20 V/V%) glycerol stock at -80 °C at the Marine Biodiscovery Centre, University of Aberdeen.[2–5]

4.2. Cultivation

From the glycerol stock, 100 μL of *Dermacoccus abyssi* MT1.1[T] cell suspension was added to 25 mL of 20 g L^{-1} NaCl (Thermo

This journal is © The Royal Society of Chemistry 2024

Org. Biomol. Chem., 2024, **22**, 6156–6165 | **6161**

Fischer Scientific) supplemented ISP2 (yeast extract 4 g, α-D-glucose 10 g, malt extract 10 g, MilliQ water 1 L, pH 7.0) seed culture. It was grown in 50 mL Falcon tubes while being shaken at a speed of 150 rpm, at 28 °C for five days. An aliquot of 1500 μL L^{-1} seed culture was inoculated into ISP2 resulting in 6 × 1 L ISP2 (yeast extract 4 g, α-D-glucose 10 g, malt extract 10 g, MilliQ water 1 L, pH 7.0) supplemented with 35 g L^{-1} ocean salt (H_2Ocean + Pro Formula with trace elements, The Aquarium Solution Ltd, Hainault Industrial Estate, Ilford Essex, UK). Erlenmeyer flasks (2 L) were sealed with a cotton-wool swab ball and with plastic tape on the top to limit oxygenation from the atmosphere.

The bacterial large-scale cultures were grown in an incubator with a transparent glass cover under ambient laboratory light conditions (ceiling lights in the laboratory above the incubator were Osram HE14W/840Lumilux Cool White 16 kW h per 1000 h, and the laboratory light switch was operated by a movement sensor, providing light ~12–14 hours a day) at 28 °C with 150 rpm for fourteen days.[5]

4.3. Extraction/isolation

After the fourteen days of cultivation the media were harvested with 50 g L^{-1} Diaion HP20 resin (>250 μm, Alfa Aesar by Thermo Fisher Scientific, Heysham, Lancashire, UK). Subsequently the crude material was subjected to Kupchan liquid–liquid partitioning. The dichloromethane fraction (FD) was partitioned further with column chromatography and HPLC to obtain dermacozines B, E, F, O, P and PCA as follows, as described in ref. 4 and 5:

Dermacozine B was obtained as yellowish-brown amorphous powder, through size exclusion chromatography of the FD fraction. Sephadex as a stationary phase was loaded onto a glass column (Quickfit, r = 0.85 cm, L = 72 cm). With CH_2Cl_2 : CH_3OH = 1 : 1 mobile phase, thirteen fractions were obtained in 15 mL vials with around ~1.4 mL min^{-1} flow rate. Fractions 9 and 10 gave dermacozine B.

Dermacozine E was obtained as purple amorphous powder, from the S4 silica fraction of the FD Kupchan fraction with HPLC chromatography with a H_2O–CH_3OH solvent system (Thermo Fischer Scientific, UK, HPLC grade) from 40% CH_3OH to 100% CH_3OH gradient over 45 min with 0.1% TFA (Thermo Fischer Scientific, UK), flow rate 1.4 mL min^{-1}, ACE HL C_{18} reversed phase column (5 μm; 250 × 10 mm), RT = 12.2 min.

Dermacozine F was obtained as bluish-purplish amorphous powder, from the S3 silica fraction with HPLC chromatography. A H_2O–CH_3OH (Thermo Fischer Scientific, UK, HPLC grade) solvent system was used with 60% CH_3OH isocratic elution over 35 min, 0.1% TFA (Thermo Fischer Scientific, UK), flow rate 1.8 mL min^{-1}, Sunfire C_{18} reversed phase column (5 μm; 250 × 10 mm), RT = 31.8 min.

Dermacozine O was obtained as ink-blue amorphous powder, from the combined S5–S8 silica fractions (based on TLC) then purified with HPLC chromatography. A H_2O–CH_3OH (Thermo Fischer Scientific, UK, HPLC grade) solvent system was used with 60% CH_3OH isocratic elution over 40 min, 0.1% TFA (Thermo Fischer Scientific, UK), flow rate 1.8 mL min^{-1}, Sunfire C_{18} reversed phase column (5 μm; 250 × 10 mm), RT = 31.9 min.

Dermacozine P was obtained as purplish amorphous powder (became greyish coloured in DMSO-d_6) from the S4 silica fraction of the FD Kupchan fraction with HPLC chromatography with a H_2O–CH_3OH solvent system (Thermo Fischer Scientific, UK, HPLC grade) from 40% CH_3OH to 100% CH_3OH gradient over 45 min with 0.1% TFA (Thermo Fischer Scientific, UK), flow rate 1.4 mL min^{-1}, ACE HL C_{18} reversed phase column (5 μm; 250 × 10 mm), RT = 15.9 min.

PCA (phenazine-1-carboxylic acid) was obtained from the S2 silica fraction through HPLC chromatography with 75% CH_3OH to 100% CH_3OH gradient over 45 min with 0.1% TFA (Thermo Fischer Scientific, UK), flow rate 1.4 mL min^{-1}, Sunfire C_{18} reversed phase column (5 μm; 250 × 10 mm), RT = 23.2 min.

High-performance-liquid-chromatography was carried out with semi-preparative gradient Agilent HPLC apparatus (1100 series), Agilent—Santa Clara, equipped with a binary pump and a diode array detector (G1315B), Agilent—Santa Clara, and the reversed phase columns are detailed in each separation description. Peak detection and the UV–Vis trace analysis were carried out at the wavelengths of 250 ± 5 nm, 280 ± 5 nm, 400 ± 25 nm, 550 ± 25 nm, and 600 ± 25 nm.

4.4. Structure determination

The isolates were subjected to (LC)-HRESI-MS^n and 1D ¹H-NMR and their structures were confirmed by comparing their ¹H-NMR chemical shifts, mass errors and MFs to the literature data [ESI S26–S37† and ref. 2–5].

PCA (phenazine-1-carboxylic) acid (1.9 mg), yellow amorphous powder; m/z 247.0479 [M + Na]⁺, 471.1064 [2M + Na]⁺; MF = $C_{13}H_8O_2N_2$, Δ = −0.4 ppm, DBE = 11. ¹H-NMR in DMSO-d_6: δ_H 14.5 (1H, bs); δ_H 8.54 (1H, d); δ_H 8.51 (1H, d); δ_H 8.38–8.42 (1H, m); δ_H 8.32–8.36 (1H, m); δ_H 8.04–8.13 (3H, m).

Dermacozine B (1.3 mg), reddish brown amorphous powder; m/z 387.1447 [M + H]⁺, 409.1279 [M + Na]⁺, 772.2753 [2M]⁺, 795.2661 [2M + Na]⁺; MF = $C_{22}H_{18}O_3N_4$, Δ = −1.18 ppm, DBE = 16. ¹H-NMR in DMSO-d_6: δ_H 7.43 (2H, bs); δ_H 6.69 (1H, d); δ_H 6.58 (2H, td); δ_H 6.50 (1H, d); δ_H 10.28 (1H, brs); δ_H 7.78 (1H, brs); δ_H 7.39 (1H, brs); δ_H 7.71 (2H, d); δ_H 7.53 (2H, t); δ_H 7.63 (1H, d); δ_H 8.07 (1H, brs); δ_H 2.95 (3H, s).

Dermacozine E (0.9 mg), bluish violet amorphous powder; m/z 397.1300 [M + H]⁺, 419.1116 [M + Na]⁺, 793.2529 [2M + H]⁺, 815.2345 [2M + Na]⁺, MF = $C_{23}H_{16}O_3N_4$, Δ = 1.14 ppm, DBE = 18. ¹H-NMR in DMSO-d_6: δ_H 11.25 (1H, brs); δ_H 8.83 (1H, brs); δ_H 8.02 (1H, d); δ_H 7.95 (1H, d); δ_H 7.84 (1H, brs); δ_H 7.78 (1H, td); δ_H 7.48 (2H, m); δ_H 7.43 (1H, m); δ_H 7.30 (3H, m); δ_H 7.20 (1H, d); δ_H 3.70 (3H, s).

Dermacozine F (1.5 mg), bluish violet amorphous powder; m/z 398.1130 [M + H]⁺, MF = $C_{23}H_{15}O_4N_3$, Δ = 1.5 ppm, DBE = 18. ¹H-NMR in DMSO-d_6: δ_H 8.73 (1H, brs); δ_H 8.06 (2H, t); δ_H 7.86 (2H, m); δ_H 7.50 (2H, t); δ_H 7.45 (1H, t); δ_H 7.37 (3H, d); δ_H 7.21 (1H, d); 3.81 (3H, s).

6162 | *Org. Biomol. Chem.*, 2024, **22**, 6156–6165

This journal is © The Royal Society of Chemistry 2024

Dermacozine O‡ (3.1 mg), ink blue amorphous powder; m/z 398.1125 $[M + H]^+$, MF = $C_{23}H_{15}O_4N_3$, Δ = 2.6 ppm, DBE = 18. ^{1}H-NMR in DMSO-d_6: δ_H 11.28 (1H, brs); δ_H 7.87 (1H, dd); δ_H 7.78 (1H, td); δ_H 7.97 (1H, dd); δ_H 7.22 (1H, d); δ_H 7.25 (1H, d); δ_H 7.31 (2H, dd); δ_H 7.47 (2H, td); δ_H 7.41 (1H, td); 3.68 (3H, s), –COOH proton not visualized.

Dermacozine P‡ (3.4 mg), purplish amorphous powder, changes to grey in DMSO-d_6, m/z 372.0992 $[M + H]^+$, MF = $C_{21}H_{13}O_4N_3$, Δ = 3.49 ppm, DBE = 17, ^{1}H-NMR in DMSO-d_6: δ_H 8.03 (1H, brs); δ_H 9.47 (1H, brs); δ_H 8.74 (1H, dd); δ_H 8.21 (1H, td); δ_H 8.55 (1H, dd); δ_H 8.95 (1H, d); δ_H 8.65 (1H, d); δ_H 7.95 (2H, dd); δ_H 7.66 (2H, td); δ_H 7.78 (1H, td), –COOH proton not observed.

4.5. Cyclic voltammetry of dermacozines

A boron doped diamond (BDD) working electrode (WE), a carbon counter electrode (CE), and a Ag quasi-reference electrode (RE) as printed electrodes were obtained from Metrohm Ltd capable of handling approx. 10–50 μL volume of sample. NaClO$_4$·H$_2$O was purchased from Sigma Aldrich, UK. Blanks of the supporting electrolyte of 0.1 M NaClO$_4$ in CH$_3$CN solution were scanned initially. Faradaic current occurred under −1.2 V and above +1.5 V, and therefore the scan window of −1.1 V to +1.4 V was investigated. The isolated compounds were prepared as cyclic voltammetry analytes as follows: 1 M NaClO$_4$ stock solution in CH$_3$CN as the supporting electrolyte for the cyclic voltammetry was prepared. The isolated dermacozines (B, E, F, O, P, and PCA) were dissolved in 1 mL CH$_3$CN in Eppendorf tubes. An aliquot of stock electrolyte solution was mixed with CH$_3$CN and the analyte resulting in 150 μL of 2.9 mM dermacozine B + 0.1 M NaClO$_4$ in CH$_3$CN, 150 μL of 3.4 mM dermacozine F + 0.1 M NaClO$_4$ in CH$_3$CN, 150 μL of 2.5 mM dermacozine O + 0.1 M NaClO$_4$ in CH$_3$CN, 150 μL of 2.6 mM dermacozine E + 0.1 M NaClO$_4$ in CH$_3$CN, 150 μL of 2 mM dermacozine P + 0.1 M NaClO$_4$ in CH$_3$CN and 150 μL of 2 mM phenazine-1-carboxylic acid + 0.1 M NaClO$_4$ in CH$_3$CN solution. The evaporation and leakage of the analyte was controlled with a rubber O-ring and a piece of parafilm on the top of the O-ring. Cyclic voltammetry scans were run at 298 K with scan rates between 50 and 100 mV s^{-1}. They were repeated in triplicate with new 50 μL analyte and a new electrode on each occasion.

4.6. Electron paramagnetic resonance spectroscopy (EPR)

The EPR spectra were recorded with an FA300 ESR Spectrometer (University of Aberdeen, UK). When dermacozine E was meticulously dried in a freeze-drier for three days, in freshly opened CHCl$_3$ solvent no radical formation was detected by EPR. However, when ~5 μL of H$_2$O was added to its solution, we observed the formation of the dermacozine E semiquinone radical. No such experiment was carried out with

dermacozine O. In the case of dermacozine E ~0.4 mg substance was dissolved in 100 μL of He bubbled CHCl$_3$ with a He gas atmosphere above the solution. For investigating dermacozine O, ~0.8 mg substance was dissolved in 100 μL CHCl$_3$ under the same conditions as for dermacozine E initially, and then the atmosphere was changed to air to see if the radical remains stable. After confirming stability in air, H$_2$O was added in 2.5 μL increments up to 7.5 μL per 100 μL CHCl$_3$ with and without irradiation. Dermacozines E and O were irradiated through a 550 ± 50 nm filter. Initially the EPR spectra of dermacozines E and O were recorded at 298 K under a He atmosphere, and the reaction with H$_2$O was recorded under normal atmospheric conditions. We were unable to record the spectra of dermacozines B, P and PCA, as they were only soluble in methanol or acetonitrile and the spectrophotometer could not be tuned with those solvent systems due to their high dielectric constant. We had insufficient material of dermacozine F left to get any other measurement done.

Author contributions

B. J. and M. J. were responsible for the cultivation of *Dermacoccus abyssi* MT1.1^T and isolation and structure determination of dermacozines. A. C. C. supervised and led the electro-chemistry methodology. R. F. H. managed the EPR methodology, the EPR measurements and the EPR spectrum modelling of dermacozines E and O. Conceptualisation of the dermacozine light-dependent photo-redox system, the linear regression model of the electrochemically derived and optical HOMO–LUMO energies, CV measurements and translation of potentials of dermacozines to SHE, with the prediction of water photocatalytic energies included, the theoretical dermacozine redox connection to the respiratory chain of *Dermacoccus abyssi* MT1.1^T and MT1.2, and further conceptualisation of the paramagnetic features and reactivity of dermacozines were carried out by B. J. The analysis was carried out by B. J., M. J., A. C. C. and R. F. H. Validation and curation were done by M. J., A. C. C., R. F. H. and B. J. Funding acquisition was carried out by M. J., A. C. C., R. F. H. and B. J. The original manuscript writing and preparation were carried out by B. J., M. J., R. F. H and A. C. C. B. J., M. J., A. C. C. and R. F. H. participated in writing—reviewing and editing the manuscript. All authors have read and agreed to the final version of the manuscript.

Data availability

UV-Vis spectroscopic data utilised for this manuscript can be found at **https://doi.org/10.1039/C001445A** for dermacozines A–G, at **https://doi.org/10.1021/np400952d** for dermacozines H–J, at **https://doi.org/10.3390/md18030131** for dermacozine M, and at **https://doi.org/10.3390/md19060325** for dermacozines N–P. Please find data source references in the 'References' section.

---

‡N.B. identical spectral data of dermacozines O and P are provided in the ESI† which have already been published in ref. 5. However, for clarity and for completeness the authors present them in the ESI† with the appropriate citation.

This journal is © The Royal Society of Chemistry 2024

Org. Biomol. Chem., 2024, **22**, 6156–6165 | **6163**

Conflicts of interest

There are no conflicts to declare.

Acknowledgements

References

1 W. Pathom-Aree, Y. Nogi, I. C. Sutcliffe, A. C. Ward, K. Horikoshi, A. T. Bull and M. Goodfellow, *Dermacoccus abyssi* sp. nov., a piezotolerant actinomycete isolated from the Mariana Trench, *Int. J. Syst. Evol. Microbiol.*, 2006, **56**, 1233–1237, DOI: **10.1099/ijs.0.64133-0**.

2 W. M. Abdel-Mageed, B. F. Milne, M. Wagner, M. Schumacher, P. Sandor, W. Pathom-Aree, M. Goodfellow, A. T. Bull, K. Horikoshi and R. Ebel, Dermacozines, a new phenazine family from deep-sea dermacocci isolated from a Mariana Trench sediment, *Org. Biomol. Chem.*, 2010, **8**, 2352–2362, DOI: **10.1039/C001445A**.

3 M. Wagner, W. M. Abdel-Mageed, R. Ebel, A. T. Bull, M. Goodfellow, H.-P. Fiedler and M. Jaspars, Dermacozines H–J Isolated from a Deep-Sea Strain of *Dermacoccus abyssi* from Mariana Trench Sediments, *J. Nat. Prod.*, 2014, **77**, 416–420, DOI: **10.1021/np400952d**.

4 W. M. Abdel-Mageed, B. Juhasz, B. Lehri, A. S. Alqahtani, I. Nouioui, D. Pech-Puch, J. N. Tabudravu, M. Goodfellow, J. Rodríguez and M. Jaspars, Whole Genome Sequence of *Dermacoccus abyssi* MT1.1 Isolated from the Challenger Deep of the Mariana Trench Reveals Phenazine Biosynthesis Locus and Environmental Adaptation Factors, *Mar. Drugs*, 2020, **18**, 131, DOI: **10.3390/md18030131**.

5 B. Juhasz, D. Pech-Puch, J. N. Tabudravu, B. Cautain, F. Reyes, C. Jiménez, K. Kyeremeh, M. Jaspars and

6 N. Dermacozine, The First Natural Linear Pentacyclic Oxazinophenazine with UV–Vis Absorption Maxima in the Near Infrared Region, along with Dermacozines O and P Isolated from the Mariana Trench Sediment Strain *Dermacoccus abyssi* MT 1.1[T], *Mar. Drugs*, 2021, **19**, 325, DOI: **10.3390/md19060325**.

6 Y. Wang and D. K. Newman, Redox Reactions of Phenazine Antibiotics with Ferric (Hydr) oxides and Molecular Oxygen, *Environ. Sci. Technol.*, 2008, **42**(7), 2380–2386, DOI: **10.1021/es702290a**.

7 M. E. Hernandez, A. Kappler and K. D. Newman, Phenazines and Other Redox-Active Antibiotics Promote Microbial Mineral Reduction, *Appl. Environ. Microbiol.*, 2004, **70**, 921–928, DOI: **10.1128/AEM.70.2.921-928.2004**.

8 M. Muller and N. D. Merrett, Pyocyanin Production by *Pseudomonas aeruginosa* Confers Resistance to Ionic Silver, *Antimicrob. Agents Chemother.*, 2014, **58**, 9, DOI: **10.1128/AAC.03069-14**.

9 S. Sinha, X. Shen, F. Galazzi, Q. Li, J. W. Zmijewski, J. R. Lancaster and K. S. Gates, Generation of Reactive Oxygen Species Mediated by 1-Hydroxyphenazine, a Virulence Factor of *Pseudomonas aeruginosa*, *Chem. Res. Toxicol.*, 2015, **28**, 175–181, DOI: **10.1021/tx500259s**.

10 L. E. P. Dietrich, C. Okegbe, A. Price-Whelan, H. Sakhtah, R. C. Hunter and K. D. Newman, Bacterial Community Morphogenesis Is Intimately Linked to the Intracellular Redox State, *J. Bacteriol.*, 2013, **195**(7), 1371, DOI: **10.1128/JB.02273-12**.

11 H. Huang, L. Sun, K. Bi, G. Zhong and M. Hu, The Effect of Phenazine-1-Carboxylic Acid on the Morphological, Physiological, and Molecular Characteristics of *Phellinus noxius*, *Molecules*, 2016, **21**, 613, DOI: **10.3390/molecules21050613**.

12 D. K. Morales, N. Grahl, C. Okegbe, L. E. Dietrich, N. J. Jacobs and D. A. Hogan, Control of *Candida albicans* metabolism and biofilm formation by *Pseudomonas aeruginosa* phenazines, *mBio*, 2013, **4**, e00526–e00512, DOI: **10.1128/mBio.00526-12**.

13 E. B. Kearney and T. P. Singer, Studies on Succinic Dehydrogenase, *J. Biol. Chem.*, 1956, **219**(2), 963–975, DOI: **10.1016/S0021-9258(18)65755-2**.

14 L. Hederstedt and L. Rutberg, Succinate Dehydrogenase – A Comparative Review, *Microbiol. Rev.*, 1951, **45**(4), 542–555 **https://journals.asm.org/doi/pdf/10.1128/mr.45.4.542-555.1981**.

15 B. A. C. Ackrell, E. B. Kearney, C. J. Coles, T. P. Singer, H. Beinert, Y.-P. Wan and K. Folkers, Kinetics of the re-oxidation of succinate dehydrogenase, *Arch. Biochem. Biophys.*, 1977, **182**(1), 107–117, DOI: **10.1016/0003-9861(77)90288-0**.

16 D. H. Park, M. Laivenieks, M. V. Guettler, M. K. Jain and J. G. Zeikus, Microbial utilization of electrically reduced neutral red as the sole electron donor for growth and metabolite production, *Appl. Environ. Microbiol.*, 1999, **65**(7), 2912–2917, DOI: **10.1128/AEM.65.7.2912-2917.1999**.

17 T. D. Harrington, V. N. Tran, A. Mohamed, R. Renslow, S. Biria, L. Orfe, D. R. Call and H. Beyenal, The mechanism of neutral red-mediated microbial electrosynthesis in

6164 | *Org. Biomol. Chem.*, 2024, **22**, 6156–6165

This journal is © The Royal Society of Chemistry 2024

Escherichia coli: menaquinone reduction, *Bioresour. Technol.*, 2015, **192**, 689–695, DOI: **10.1016/j. biortech.2015.06.037**.

18 I. Ledezma-Yanez, O. Díaz-Morales, M. C. Figueiredo and M. T. M. Koper, Hydrogen Oxidation and Hydrogen Evolution on a Platinum Electrode in acetonitrile, *ChemElectroChem*, 2015, **2**(10), 1612–1622, DOI: **10.1002/ celc.201500341**.

19 V. Fourmond, P. A. Jacques, M. Fontecave and V. Artero, *Inorg. Chem.*, 2010, **49**, 10338–10347, DOI: **10.1021/ ic101187v**.

20 W. R. Fawcett, The Ionic Work Function and its Role in Estimating Absolute Electrode Potentials, *Langmuir*, 2008, **24**(17), 9868–9875, DOI: **10.1021/la7038976**.

21 C. De la Cruz, A. Molina, N. Patil, E. Ventosa, R. Marcilla and A. Mavrandonakis, New insights into phenazine-based organic redox flow batteries by using high-throughput DFT modelling, *Sustainable Energy Fuels*, 2020, **4**, 5513–5521, DOI: **10.1039/D0SE00687D**.

22 W. S. Zaugg, Spectroscopic Characteristics and Some Chemical Properties of *N*-Methylphenazonium Methyl Sulfate (Phenazine Methosulphate) and Pyocyanine at the Semiquinoid Oxidation Level, *J. Biol. Chem.*, 1964, **239**(11), 3964–3970, DOI: **10.1016/S0021-9258(18)91229-9**.

23 E. Tsoo, King Reconstitution of Respiratory Chain Enzyme Systems: XI. Use of artificial electron acceptors in the assay of Succinate-Dehydrogenating Enzymes, *J. Biol. Chem.*, 1963, **238**, 4032–4036, DOI: **10.1016/S0021-9258(18)51825-1**.

24 W. J. Catallo, J. B. Fleix and R. J. Gale, Movement of methyl-phenazyl free radicals in polar and nonpolar liquids, *Free Radicals Biol. Med.*, 1992, **13**(1), 35–40, DOI: **10.1016/0891-5849(92)90163-B**.

25 K. H. Hausser, Stickstoff-Radikale bei tiefen Temperaturen I. *N*-Äthyl-phenazyl, *Naturwissenschaften*, 1956, **43**, 14–15, DOI: **10.1007/BF00601174**.

26 K. H. Hausser and L. Birkofer, Negative Thermochromie des *N*-Äthyl-phenazyl-Radikals, *Naturwissenschaften*, 1955, **42**(4), 97–97, DOI: **10.1007/BF00617244**.

27 M. J. Hopwood, I. Rapp, C. Schlosser and E. P. Achterberg, Hydrogen peroxide in deep waters from the Mediterranean Sea, South Atlantic and South Pacific Oceans, *Sci. Rep.*, 2017, **7**(7), 43436, DOI: **10.1038/srep43436**.

28 G. M. Belyaev, *Deep-sea Ocean trenches and Their Fauna*, Nauka, Moscow, 1989. **https://escholarship.org/uc/item/46n6148x**.

29 K. Fukui, The Role of Frontier Orbitals in Chemical Reactions, *Science*, 1982, **218**(4574), 747–754, DOI: **10.1126/ science.218.4574.747**.

30 M. Martínez-Cifuentes, R. Salazar, O. Ramírez-Rodríguez, B. Weiss-López and R. Araya-Maturana, Experimental and Theoretical Reduction Potentials of Some Biologically Active ortho-Carbonyl para-Quinones, *Molecules*, 2017, **22**(4), 577, DOI: **10.3390/molecules22040577**.

31 A. Franco, A. Chukwubuikem, C. Meiners and M. A. Rosenbaum, Exploring phenazine electron transfer interaction with elements of the respiratory pathways of *Pseudomonas putida* and *Pseudomonas aeruginosa*, *Bioelectrochemistry*, 2024, **157**, 108636, DOI: **10.1016/j. bioelechem.2023.108636**.

32 A. Castellano, J.-P. Catteau and A. Lablache-Combier, Mechanism of Formation of Semiquinone Radicals by Ultraviolet Irradiation of Six-membered Aromatic Aza-compounds in Neutral Methanol, and of Radical Cations by Ultra-Violet Irradiation of Six-membered Aromatic Diaza-compounds in Methanol acidified with Hydrochloric acid, *J. Chem. Soc., Chem. Commun.*, 1972, **22**, 1207–1208, DOI: **10.1039/C39720001207**.

33 W. S. Zaugg, L. P. Vernon and A. Tirpack, Photoreduction of Ubiquinone and Photooxidation of Phenazine Methosulphate by Chromatophores of Photosynthetic Bacteria and Bacteriochlorophyll, *Proc. Natl. Acad. Sci. U. S. A.*, 1964, **51**, 232–238, DOI: **10.1073/pnas.51.2.232**.

34 B. Milne, P. Norman, F. Nogueira and C. Cardoso, Marine natural products from the deep Pacific as potential non-linear optical chromophores, *Phys. Chem. Chem. Phys.*, 2013, **15**, 14814, DOI: **10.1039/C3CP52528G**.

35 E. Ciarrocchi and N. Belcari, Cerenkov luminescence imaging: physics principles and potential applications in biomedical sciences, *EJNMMI Phys.*, 2017, **4**, 14, DOI: **10.1186/s40658-017-0181-8**.

36 G. T. Reynolds and R. A. Lutz, Sources of Light in the Deep Ocean, *Rev. Geophys.*, 2001, **39**, 123–136, DOI: **10.1029/ 1999RG000071**.

37 R. Nakagawa and Y. Nishina, Simulating the redox potentials of unexplored phenazine derivatives as electron mediators for biofuel cells, *J. Phys. Energy*, 2021, **3**, 034008, DOI: **10.1088/2515-7655/abebc8**.

38 M. Schumacher, M. Kelkel, M. Dicato and M. Diederich, A Survey of Marine Natural Compounds and Their Derivatives with Anti-Cancer Activity Reported in 2010, *Molecules*, 2011, **16**, 5629–5646, DOI: **10.3390/molecules16075629**.

39 V. R. Ghanta, N. Madala, A. Pasula, S. K. S. S. Pindiprolu, K. S. Battula, P. T. Krishnamurthy and B. Raman, Novel dermacozine-1-carboxamides as promising anticancer agents with tubulin polymerization inhibitory activity, *RSC Adv.*, 2019, **9**, 18670–18677, DOI: **10.1039/C9RA02416F**.

40 R. Combuca da Silva Junior, K. da Silva Souza Campanholi, F. Amanda Pedroso de Morais, L. Adriane de Moraes Pinto, F. dos Santos Rando, M. Soares dos Santos Pozza and W. Caetano, *Phenazines and Photoactive Formulations: Promising Photodrugs for Photodynamic Therapy*, IntechOpen, 2023. DOI: **10.5772/intechopen.110588**.

41 S. J. Beech, S. Noimark, K. Page, N. Noor, E. Allan and I. P. Parki, Incorporation of crystal violet, methylene blue and safranin O into a copolymer emulsion; the development of a novel antimicrobial paint, *RSC Adv.*, 2015, **5**, 26364–26375, DOI: **10.1039/C5RA01673H**.

42 T. V. Verissimo, N. T. Santos, J. R. Silva, R. B. Azevedo, A. J. Gomes and C. N. Lunardi, *In vitro* cytotoxicity and phototoxicity of surface-modified gold nanoparticles associated with neutral red as a potential drug delivery system in phototherapy, *Mater. Sci. Eng., C*, 2016, **65**, 199–204, DOI: **10.1016/j.msec.2016.04.030**.

This journal is © The Royal Society of Chemistry 2024

Org. Biomol. Chem., 2024, **22**, 6156–6165 | **6165**